Viability of the matter bounce scenario in Loop Quantum Cosmology from BICEP2 last data

Jaume de Haro* and Jaume Amorós†
Departament de Matemàtica Aplicada I, Universitat Politècnica de Catalunya, Diagonal 647, 08028 Barcelona, Spain

The CMB map provided by the *Planck* project constrains the value of the ratio of tensor-to-scalar perturbations, namely r, to be smaller than 0.11 (95 % CL). This bound rules out the simplest models of inflation. However, recent data from BICEP2 is in strong tension with this constrain, as it finds a value $r = 0.20^{+0.07}_{-0.05}$ with $r = 0$ disfavored at 7.0σ, which allows these simplest inflationary models to survive. The remarkable fact is that, even though the BICEP2 experiment was conceived to search for evidence of inflation, its experimental data matches correctly theoretical results coming from the matter bounce scenario (the alternative model to the inflationary paradigm). More precisely, most bouncing cosmologies do not pass *Planck's* constrains due to the smallness of the value of the tensor/scalar ratio $r \leq 0.11$, but with new BICEP2 data some of them fit well with experimental data. This is the case with the matter bounce scenario in the teleparallel version of Loop Quantum Cosmology.

PACS numbers: 04.80.Cc, 98.80.Bp, 98.80.Qc, 04.60.Pp

1. Introduction.— The latest *Planck* temperature data for cosmic inflation constrains the spectral index for scalar perturbations to be $n_s = 0.9603 \pm 0.0073$, ruling out exact scale invariance with over 5σ confidence, and establishes an upper bound for tensor/scalar ratio given by $r \leq 0.11$ (95 % CL) [1]. Such data shrinks the set of allowed simplest inflationary models: power law potentials in chaotic inflation [2], exponential potential models [3], inverse power law potentials [4], are disfavored because they do not provide a good fit to *Planck's* data [1, 5]. In fact, this data set prefers a subclass of inflationary models with *plateau-like* inflation potentials (see for example [6]) and R^2 gravity [7].

On the other hand, recent results from the BICEP2 experiment [8], designed to look for the signal of gravitational waves in the B-mode power spectrum, lead to the same constrain for the spectral index, but constrain the ratio of tensor-to-scalar perturbations to be $r = 0.20^{+0.07}_{-0.05}$ with $r = 0$ disfavored at 7.0σ (see figure 13 of [8] to compare *Planck's* with BICEP2 data). This higher value of r extends the set of compatible inflationary models, allowing back some of the simplest inflationary models cited above.

Dealing with the matter bounce scenario, the alternative to the inflationary paradigm (see [9] for a report about bouncing cosmologies), one encounters a similar problem when one tries to match *Planck's* data with theoretical results: theoretical results provide, in general, values of r higher than 0.11 and, then, to sort out this problem some very complicated mechanism has to be introduced to enhance the power spectrum of scalar perturbations [10], reducing the ratio r enough to achieve the bound 0.11. However, the higher value of r provided by BICEP2 allows the viability of some of bouncing models. In particular, it allows the viability of the matter bounce scenario in Loop Quantum Cosmology (LQC) when the potential chosen is the simplest one. More precisely: we will calculate, for matter bounce scenario, the spectral index and the tensor/scalar ratio coming from holonomy corrected LQC (the perturbative theory obtained replacing the Ashtekar connection by a suitable sinus function and inserting counter-terms to preserve the algebra of constrains [11]) and teleparallel LQC (the perturbative $F(T)$ theory applied to the model that, in flat Friedmann-Robertson-Walker geometry, coincides with LQC [12]), and we will check that in the case of teleparallel LQC they match correctly with BICEP2 data, and for holonomy corrected LQC they match correctly with *Planck's* data. However, results coming from holonomy corrected LQC have to be taken with caution because the way to calculate tensor perturbations in this theory is not unambiguously defined [12], leading to different values for the tensor/scalar ratio.

The units used in the letter are $\hbar = c = 8\pi G = 1$.

Constrains on inflationy models from experimental data.— Slow-roll inflation is essentially based in two parameters [13]:

$$\epsilon = -\frac{\dot{H}}{H^2} \quad \text{and} \quad \eta = 2\epsilon - \frac{\dot{\epsilon}}{2H\epsilon}, \tag{1}$$

which in the slow-roll phase, i.e., when the dynamics of the system is given by equations

$$H^2 \cong \frac{V(\bar{\varphi})}{3} \quad \text{and} \quad 3H\dot{\bar{\varphi}} + V_{\bar{\varphi}} \cong 0, \tag{2}$$

where $\bar{\varphi}(t)$ is the homogeneous part of the scalar field, are given by

$$\epsilon \cong \frac{1}{2}\left(\frac{V_{\bar{\varphi}}}{V}\right)^2 \quad \text{and} \quad \eta \cong \frac{V_{\bar{\varphi}\bar{\varphi}}}{V}. \tag{3}$$

Using slow-roll parameters ϵ and η the spectral index for scalar perturbations and the ratio of tensor-to-scalar perturbations are given by

$$n_s \cong 1 + 2\eta - 6\epsilon \quad \text{and} \quad r \cong 16\epsilon. \tag{4}$$

To compare theoretical results with current observations we need the number of e-folds during inflation, namely N, which

*E-mail: jaime.haro@upc.edu
†E-mail: jaume.amoros@upc.edu

in slow-roll approximation is given by

$$N=\int_{t_b}^{t_e} H dt \cong \int_{\bar\varphi_e}^{\bar\varphi_b} \frac{V}{V_{\bar\varphi}} d\bar\varphi, \tag{5}$$

where the sub-index b (resp. e) refers to the beginning (resp. end) of inflation.

As a first example to compare theoretical with experimental results, we choose a power law potential $V(\bar\varphi)=\lambda\bar\varphi^n$. For this potential one has

$$n_s \cong 1-\frac{n(n+2)}{\bar\varphi_b^2}, r\cong \frac{8n^2}{\bar\varphi_b^2} \text{ and } N\cong \frac{2\bar\varphi_b^2-n^2}{4n}, \tag{6}$$

where we have chosen as the end of inflation the condition $\epsilon=1$, which is equivalent to $\bar\varphi_e^2=\frac{n^2}{2}$, and to calculate n_s and r we have evaluated ϵ and η at the beginning of inflation.

Removing $\bar\varphi_b^2$ in (6), i.e., writing n_s and r in terms of the number of e-folds, one gets

$$n_s \cong 1-\frac{2(n+2)}{4N+n}, r\cong \frac{16n}{4N+n} \Longrightarrow n_s\cong 1-\frac{n+2}{8n}r. \tag{7}$$

In the case of a quadratic potential $n=2$, for 60 e-folds, the minimum needed to solve the horizon and flatness problems [14], one gets $n_s=0.9669$ and $r=0.132$. When one increases the number of e-folds, n_s increases and r decreases. Then, for the maximal allowed value of the spectral index $n_s=0.9676$ one has $r=0.1296$, which means that the model with a quadratic potential does not fit well neither with *Planck's* nor with BICEP2 data.

In the same way, since r increases as long as the parameter n increases, one can conclude that inflationary power law models are disfavored by $Planck's$ data.

However, using BICEP2 data, the model $n=4$ with 70 e-folds is acceptable because it satisfies $n_s=0.9577$ and $r=0.2253$. To be more specific, from the third equation of (7) r is constrained to belong in the interval

$$\left(\frac{8n}{n+2}\times 0.0324, \frac{8n}{n+2}\times 0.047\right).$$

Then, potentials with $n=3,4$ and 5 are allowed by BICEP2 data, because r belongs in the interval $(0.15, 0.27)$.

As a second example we consider R^2 gravity, where one has [7]

$$n_s=1-\frac{2}{N}, r=\frac{12}{N^2} \Longrightarrow n_s=1-\sqrt{\frac{r}{3}}. \tag{8}$$

Using the data $n_s=0.9603\pm 0.0073$ and equation (8) one obtains the constrain

$$0.0031\leq r\leq 0.0066,$$

what means that BICEP2 data disregards this model. However, the model matches correctly with *Planck's* data. Effectively, for 60 e-folds one has $n_s=0.9666$ and $r=0,0033$ which enters perferctly in the range of values obtained from *Planck's* temperature anisotropy mesurements.

Calculation of the power spectrum in LQC.— To calculate the power spectrum of scalar perturbations for the matter bounce scenario in LQC, first of all, one has to look for a potential of the scalar field that, at early times when holonomy corrections can be disregarded, leads to a matter dominated universe. Solving the holonomy corrected Friedmann equation and the conservation equation for a matter dominated universe (see for instance [15])

$$H^2=\frac{\rho}{3}\left(1-\frac{\rho}{\rho_c}\right); \quad \dot\rho=-3H\rho, \tag{9}$$

where ρ_c is the so-called *critical density*, one obtains the following quantities [12]

$$a(t)=\left(\frac{3}{4}\rho_c t^2+1\right)^{1/3} \text{ and } \rho(t)=\frac{\rho_c}{\frac{3}{4}\rho_c t^2+1}. \tag{10}$$

To find one such potential, one can impose that the pressure vanishes, i.e., $P\equiv\frac{\dot{\bar\varphi}^2}{2}-V(\bar\varphi)=0$, which leads to the equation

$$\dot{\bar\varphi}^2(t)=\rho(t)\Longleftrightarrow \dot{\bar\varphi}^2(t)=\frac{\rho_c}{\frac{3}{4}\rho_c t^2+1}, \tag{11}$$

where we have used the third equation of (10).

This equation has the particular solution

$$\bar\varphi(t)=\frac{2}{\sqrt{3}}\ln\left(\sqrt{\frac{3}{4}\rho_c}t+\sqrt{\frac{3}{4}\rho_c t^2+1}\right), \tag{12}$$

which leads to the potential

$$V(\bar\varphi)=2\rho_c\frac{e^{-\sqrt{3}\bar\varphi}}{\left(1+e^{-\sqrt{3}\bar\varphi}\right)^2}. \tag{13}$$

It is important to realize that solution (12) is special in the sense that it satisfies for all time $\dot{\bar\varphi}^2(t)/2=V(\bar\varphi(t))$, that is, if the universe is described by this solution, it will be matter dominated dominated all the time. However, the other solutions, that is, the solutions of the conservation equation

$$\dot\rho=-3H_\pm(\rho+P)\Longleftrightarrow \ddot{\bar\varphi}+3H_\pm\dot{\bar\varphi}+V_{\bar\varphi}=0, \tag{14}$$

where the Hubble parameter is equal to $H_-=-\sqrt{\frac{\rho}{3}(1-\frac{\rho}{\rho_c})}$ in the contracting phase and $H_+=\sqrt{\frac{\rho}{3}(1-\frac{\rho}{\rho_c})}$ in the expanding one, do not lead to a matter-dominated universe. Only at early and late times the universe is matter dominated because the solution (12) is a global repeller at early times and a global attractor at late ones.

Once we have introduced the simplest potential for the matter bounce scenario in LQC, we deal with perturbations. In this scenario the power spectrum for scalar perturbations is given by [12]

$$\mathcal{P}(k)=\frac{3\rho_c^2}{\rho_{pl}}\left(\int_{-\infty}^{\infty}\frac{dt}{a(t)z^2(t)}\right)^2, \tag{15}$$

provided that $a(t) \cong \left(\frac{3}{4}\rho_c t^2\right)^{1/3}$ at early times, where we have introduced Planck's energy density $\rho_{pl} = 64\pi^2$ in our units.

In the case of holonomy corrected LQC, whose equations are obtained from the classical perturbation equations [16] replacing, like in isotropic models, the Ashtekar connection by suitable sinus functions and adding some counter-terms to avoid anomalies coming from the no preservation of the algebra of constrains [11], one has $z = \frac{a\dot{\bar\varphi}}{H}$ which for the analytic solution (12) is given by $\frac{2a^{5/2}(t)}{\sqrt{\rho_c}t}$ [17], and which leads, after a simple calculation, to

$$\mathcal{P}(k) = \frac{\pi^2}{9}\frac{\rho_c}{\rho_{pl}}. \tag{16}$$

On the other hand, in teleparallel LQC, whose perturbation equations are the ones of $F(T)$ gravity [18] applied to a model (see eq. (2.12) and (2.23) of [12]) whose teleparallel Friedmann equation coincides with the holonomy corrected one (9), one has $z = \frac{a\sqrt{|\Omega|}\dot{\bar\varphi}}{c_s H}$ where $\Omega = 1 - \frac{2\rho}{\rho_c}$ and the square of the velocity of sound is given by [12]

$$c_s^2 \equiv |\Omega| \frac{\arcsin\left(2\sqrt{\frac{3}{\rho_c}}H\right)}{2\sqrt{\frac{3}{\rho_c}}H}. \tag{17}$$

For the particular solution (12) one has

$$z(t) = 2\left(\frac{3}{\rho_c}\right)^{1/4} \frac{a(t)|t|^{1/2}}{t\sqrt{\arcsin\left(\frac{\sqrt{3\rho_c}|t|}{a^3(t)}\right)}}, \tag{18}$$

giving as a power spectrum

$$\mathcal{P}(k) = \frac{16}{9}\frac{\rho_c}{\rho_{pl}}\mathcal{C}^2, \tag{19}$$

where $\mathcal{C} \cong 0.9159$ is Catalan's constant.

This result has to be compared with the seven-year data of WMAP [19], which constrains the value of the power spectrum for scalar perturbations to be $\mathcal{P}(k) \cong 2\times 10^{-9}$, which means that, in both cases (holonomy corrected and teleparallel LQC), when one considers the solution (12), the value of the critical density has to be of the order $\rho_c \sim 10^{-9}\rho_{pl}$.

The ratio of tensor-to-scalar perturbations in LQC is given by

$$r \cong \frac{1}{6}\left(\frac{\int_{-\infty}^{\infty}\frac{1}{az_T^2}dt}{\int_{-\infty}^{\infty}\frac{1}{az^2}dt}\right)^2, \tag{20}$$

where $z_T = \frac{a}{\sqrt{\Omega}}$ in holonomy corrected LQC and $z_T = \frac{ac_s}{\sqrt{2|\Omega|}}$ in the teleparallel version.

Remark .1. *A little bit of caution is needed when one deals with with tensor perturbation in LQC, because z_T is imaginary in the super-infaltionary phase ($\rho_c/2 < \rho \le \rho_c$), leading to an abnormally small value of r. Moveover its corresponding Mukhanov-Sasaki equation (eq. 31 of [20]) is singular at $\rho = \rho_c/2$, meaning that this equation has infinitely many solutions, and consequently, in holonomy corrected LQC, the power spectrum of tensor perturbations and the tensor/scalar ratio are not unambiguously defined (see for details [12]).*

For the analytical solution (12), in holonomy corrected LQC one has $r = 0$ which is an abnormally small value, and in teleparallel LQC we have obtained the following very high value $r = 6\left(\frac{Si(\pi/2)}{\mathcal{C}}\right)^2 \cong 13.4381$, where $Si(x) \equiv \int_0^x \frac{\sin y}{y}dy$ is the Sine integral function.

However, these results do not mean that the matter bounce scenario has to be disregarded. What they mean is that, for orbits (solutions of (14)) near the solution (12), the theoretical results do not match with the current experimental data. But there will be other orbits that fit welll with data obtained from *Planck* or BICEP2.

Dealing with the spectral index, the matter bounce scenario provides a power spectrum exactly scale invariant, i.e., $n_s = 1$ not agreeing with current data, which states that is nearly scale invariant with a slight red tilt. The problem is easily solved if one assume that at early times, in the contracting phase, the universe has an state equation of the form $P = \omega\rho$ with $|\omega| \ll 1$. In LQC a potential that leads to this kind of universe is [17]

$$V(\bar\varphi) = 2\rho_c(1-\omega)\frac{e^{-\sqrt{3(1+\omega)}\bar\varphi}}{\left(1+e^{-\sqrt{3(1+\omega)}\bar\varphi}\right)^2}. \tag{21}$$

In fact, this potential provides an analytic orbit (an analytic solution of (14)) that depicts an universe whose equation of state is $P = \omega\rho$ all the time. Moreover, at early times this orbit is a repeller and at late times an attractor, meaning that all the orbits represent a universe that at early and late times has as equation of state $P = \omega\rho$. As a consequence, for all the orbits of the system the spectral index is given by [17] $n_s = 1 + 12\omega$. Then, to match with observational data one only has to choose $\omega = -0.0033 \pm 0.0006$.

Finally, is important to stress that for these small values of ω the corresponding formulae for the power spectrum and the tensor/scalar ratio do not change significatively, i.e., we can continue using formulae (15) and (20).

Numerical results.— Our numerical study is based in the numerical resolution of equation (14). To perform this calculation, one has to take into account that in LQC the orbits start at early times in the contracting phase ($H < 0$), and when its energy density reaches the critical density $\rho = \rho_c$ the universe bounces and enters in the expanding phase ($H > 0$). Then, to obtain the phase portrait of the system in the plane $(\bar\varphi, \dot{\bar\varphi})$, for any initial condition $(\bar\varphi_0, \dot{\bar\varphi}_0)$ one has to integrate numerically equation (14) with $H = H_-$ forward in time, and when the orbit reaches the curve $\rho = \rho_c$ at some point $(\bar\varphi_1, \dot{\bar\varphi}_1)$, one has to integrate numerically forward in time equation (14) with $H = H_+$ for the new initial condition $(\bar\varphi_1, \dot{\bar\varphi}_1)$. The phase portrait is pictured in figure 1.

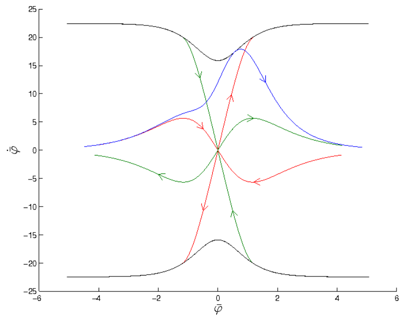

Figure 1: Phase portrait: the black curves are defined by $\rho = \rho_c$, and depict the points where the universe bounces. The point $(0, 0)$ is a saddle point, red (resp. green) curves are the invariant curves in the contracting (resp. expanding) phase. The blue curve corresponds to an orbit different from the analytically one (12). Note that, before (resp. after) the bounce the blue curve does not cut the red (resp. green) curves. It is important to realize that the allowed orbits are those that catch the black curve in the region delimited by an unstable red curve and an stable green curve, because for orbits that do not satisfy this condition, $\dot{\bar\varphi}$ vanishes at some time, meaning that its corresponding power spectrum diverges.

For a wide range of the orbits calculated numerically, we have obtained for the power spectrum of scalar perturbations, which, in the case of potential (13), is proportional to the ratio ρ_c/ρ_{pl} for all the orbits of the system (14), the following results:

1. In holonomy corrected LQC, the minimum value of $\mathcal{P}(k)$ is obtained for the orbit that at bouncing time satisfies $\bar\varphi \cong -0.9870$, for that orbit we have obtained $\mathcal{P}(k) \cong 23 \times 10^{-3} \frac{\rho_c}{\rho_{pl}}$.

2. In teleparallel LQC the orbit which gives the minimum value of the power spectrum satisfies, at bouncing time, $\bar\varphi \cong -0.9892$ and the value of the power spectrum is approximately the same as in holonomy corrected LQC $\mathcal{P}(k) \cong 40 \times 10^{-3} \frac{\rho_c}{\rho_{pl}}$.

Then for those orbits, in order to match with the current experimental result $\mathcal{P}(k) \cong 2 \times 10^{-9}$, in both theories one has to choose $\rho_c \sim 10^{-5}\rho_{pl}$ which is 4 orders greater than the value needed using the analytic solution. This result does not favour holonomy corrected LQC because the current value of the critical density, obtained relating the black hole entropy with the Bekenstein-Hawking entropy formula, is approximately $0.4\rho_{pl}$ [21]. However, it does not affect teleparellel LQC where ρ_c is merely a parameter whose value has to be obtained from observations.

We have also calculated the ratio of tensor-to-scalar perturbations, which is independent on the parameter ρ_c, for the potential (13) in teleparallel LQC using formula (20). Its value in admissible solutions (those with $\dot{\bar\varphi} \neq 0$ at all times) ranges continuously from a minimal value $r \cong 0.1243$, attained by the orbit with the universe bouncing at $\bar\varphi \cong -1.18$, to the maximal value $r \cong 13.4381$, attained by the solution (12) bouncing at $\bar\varphi = 0$. The confidence interval $r = 0.20^{+0.07}_{-0.05}$ derived from BICEP2 data is realized by solutions bouncing when $\bar\varphi \in [-1.174, -1.162]$, with the expected value $r = 0.20$ realized by bouncing at $\bar\varphi = -1.169$.

On the other hand, in holonomy corrected LQC, numerical results show that the allowed orbits provide values of r in the interval $[0, 0.06]$, matching correctly with *Planck's* constrain $r \leq 0.11$.

We thank Professor Sergei D. Odintsov for correspondance and useful comments. This investigation has been supported in part by MINECO (Spain), project MTM2011-27739-C04-01, MTM2012-38122-C03-01, and by AGAUR (Generalitat de Catalunya), contracts 2009SGR 345 and 994.

[1] P.A.R. Ade et al., (2013) [arXiv:1302.5082].
[2] A.D. Linde, Phys. Lett. **B129**, 177 (1983).
[3] F. Lucchin and S. Matarrese, Phys. Rev. **D32**, 1316 (1985).
[4] J.D. Barrow, Phys. Lett. **B235**, 40 (1990).
[5] A. Ijjas, P.J. Steinhardt and A. Loeb, Phys. Lett. **B723**, 261 (2013) [arXiv:1304.2785].
[6] K.A. Olive, Phys. Rept. **190**, 307 (1990).
[7] L. Sebastiani, G. Cognola, R. Myrzakulov, S.D. Odintsov and S. Zerbini, Phys. Rev. **D89**, 023518 (2014) [arXiv:1311.0744].
[8] P.A.R. Ade et al., (2014) [arXiv:1403.3985].
[9] R.H. Brandenberger, (2012) [arXiv:1206.4196].
[10] Y.-F Cai, R.H. Brandenberger and X. Zhang, JCAP **03** 003, (2011) [arXiv:1101.0822].
[11] T. Cailleteau, J. Mielczarek, A. Barrau and J. Grain, Class. Quant. Grav. **29** 095010, (2012) [arXiv:1111.3535].
[12] J. Haro, JCAP **11** 068, (2013) [arXiv:1309.0352].
[13] E.D. Stewart and D.H. Lyth, Phys. Lett. **B302** 171, (1993) [arXiv:9302019].
[14] A. Guth, Phys. Rev. **D23** 347, (1981).
[15] P. Singh, Class. Quant. Grav. **26** 125005, (2009) [arXiv:0901.2750].
[16] V.F. Mukhanov, H.A. Feldman and R.H. Brandenberger, Phys. Rept. **215** 203, (1992).
[17] E. Wilson-Ewing, JCAP **03** 026, (2013) [arXiv:1211.6269].
[18] Y-F. Cai, S-H. Chen, J.D. Dent, S. Dutta and E. N. Saridakis Class. Quantum Grav. 28, 215011 (2011) [arXiv:1104.4349].
[19] D. Larson et al., Astrophys. J. Suppl. **192** 16, (2011) [arXiv:1001.4635].
[20] T. Cailleteau A. Barrau, J. Grain and F. Vidotto, Phys. Rev. **D86** 087301, (2012) [arXiv:1206.6736].
[21] K.A. Meissner, Class. Quant. Grav. **21** 5245, (2004) [arXiv:0407052].